Respiratory Physiology & Neurobiology 261 (2019) 15–23

Contents lists available at ScienceDirect

Respiratory Physiology & Neurobiology

journal homepage: www.elsevier.com/locate/resphysiol

Cervical spinal contusion alters Na^+-K^+-2Cl- and K^+-Cl- cation-chloride cotransporter expression in phrenic motor neurons

Latoya L. Allen[a,b,c], Yasin B. Seven[a,c], Tracy L. Baker[d], Gordon S. Mitchell[a,c,*]

[a] Department of Physical Therapy, University of Florida, Gainesville, FL 32611 USA
[b] Department of Neuroscience, University of Florida, Gainesville, FL 32610 USA
[c] Center for Respiratory Research and Rehabilitation, University of Florida, Gainesville, FL 32611 USA
[d] Department of Comparative Biosciences, University of Wisconsin-Madison, Madison, WI 53706 USA

ARTICLE INFO

Keywords:
Phrenic motor neurons
NKCC1
KCC2
Spinal cord injury
Contusion

ABSTRACT

Spinal chloride-dependent synaptic inhibition is critical in regulating breathing and requires neuronal chloride gradients established by cation-chloride cotransporters Na^+-K^+-$2Cl^-$ (NKCC1) and K^+-Cl^- (KCC2). Spinal transection disrupts NKCC1/KCC2 balance, diminishing chloride gradients in neurons below injury, contributing to spasticity and chronic pain. It is not known if similar disruptions in NKCC1/KCC2 balance occur in respiratory motor neurons after incomplete cervical contusion (C2SC). We hypothesized that C2SC disrupts NKCC1/KCC2 balance in phrenic motor neurons. NKCC1 and KCC2 immunoreactivity was assessed in CtB-positive phrenic motor neurons. Five weeks post-C2SC: 1) neither membrane-bound nor cytosolic NKCC1 expression were significantly changed, although the membrane/cytosolic ratio increased, consistent with net chloride influx; and 2) both membrane and cytosolic KCC2 expression increased, although the membrane/cytosolic ratio decreased, consistent with net chloride efflux. Thus, contrary to our original hypothesis, complex shifts in NKCC1/KCC2 balance occur post-C2SC. The functional significance of these changes remains unclear.

1. Introduction

Cervical spinal cord injury (SCI) disrupts bulbospinal pathways to respiratory motor neurons, causing respiratory muscle paralysis and diminished breathing capacity. Respiratory insufficiency causes inadequate airway protection and/or overt ventilatory failure and is the leading cause of morbidity and mortality in people with cervical SCI (Frankel et al., 1998; NSCISC, 2018; Winslow and Rozovsky, 2003). Respiratory function in people with cervical SCI can be further compromised by respiratory muscle spasticity due to inappropriate activity during normally inactive expiratory phases (Britton et al., 2005; Laffont et al., 2003; Silver and Lehr, 1981).

Chloride-dependent synaptic inhibition is necessary for inspiratory-expiratory coordination (Tonkovic-Capin et al., 2003; Zuperku and McCrimmon, 2002). Dysregulation of chloride-dependent synaptic inhibition can lead to inappropriate activity during inspiration and expiration, reducing breathing coordination and/or respiratory neuron gain modulation (Zuperku and McCrimmon, 2002). Chloride-dependent synaptic inhibition can be dysregulated by degrading the chloride gradient necessary for hyperpolarization (Hebert et al., 2004; Price et al., 2009; Viemari et al., 2011). In mature neurons, low $[Cl^-]_i$ is maintained by a balance of inwardly directed Na^+-K^+-$2Cl^-$ cotransporter type 1 (NKCC1) and outwardly directed K^+-Cl^- cotransporter type 2 (KCC2) and is essential to the strength and polarity of fast, chloride-dependent $GABA_A$- and glycine-mediated synaptic inhibition (Delpire and Mount, 2002; Kaila et al., 2014; Payne, 1997; Rivera et al., 1999). Dysregulated chloride-dependent synaptic inhibition contributes to muscle spasticity in rodent models of spinal and peripheral nerve injury (Bos et al., 2013; Boulenguez et al., 2010; Nabekura et al., 2002), chronic pain (Coull et al., 2003; Cramer et al., 2008; Hasbargen et al., 2010) and epilepsy (Cohen et al., 2002; Kaila et al., 2014; Payne et al., 2003).

Following thoracic transection, membrane-bound KCC2 in lumbar motor neurons is decreased, resulting in increased $[Cl^-]_i$ and deterioration in the ability to elicit $GABA_A$ and glycine-mediated hyperpolarization (Boulenguez et al., 2010). This is the reverse of normal shifts in NKCC1/KCC2 balance in early development, where CNS neuronal NKCC1 is downregulated and KCC2 upregulated with increasing age; these shifts enable inhibitory chloride-dependent neurotransmission (Ben-Ari et al., 1997; Blaesse et al., 2006; Payne et al., 2003; Rivera

* Corresponding author at: University of Florida, College of Public Health & Health Professions, Department of Physical Therapy, Box 100154, UFHSC, Gainesville, FL 32610-0154, USA.
E-mail address: gsmitche@phhp.ufl.edu (G.S. Mitchell).

https://doi.org/10.1016/j.resp.2018.12.009
Received 28 July 2018; Received in revised form 21 December 2018; Accepted 23 December 2018
Available online 24 December 2018

et al., 1999). With injury, some have suggested that dysregulated chloride-dependent synaptic inhibition is an adaptive cellular response that facilitates neuronal survival by reducing the energetic costs needed to preserve low $[Cl^-]_i$ (Kaila et al., 2014). However, this potentially adaptive response may lead to allodynia (Cramer et al., 2008) or spasticity in motor systems (Boulenguez et al., 2010). In respiratory motor neurons, similar shifts in the NKCC1/KCC2 balance could help preserve phasic respiratory motor neuron activity (and breathing ability) to the greatest extent possible when medullary respiratory inputs are disrupted by cervical SCI. On the other hand, if such shifts occur following moderate C2 contusion injuries, our data suggest that they have been restored to (or even beyond) normal by 5 weeks post-injury, consistent with other populations of neurons (Cramer et al., 2008; Modol et al., 2014).

Since no information is available concerning the impact of cervical SCI on NKCC1/KCC2 balance in phrenic motor neurons, we determined the effects of unilateral C2 contusion injuries (C2SC) on membrane-bound and cytosolic NKCC1 and KCC2 expression within identified phrenic motor neurons. Our original hypothesis was that C2SC upregulates membrane-bound NKCC1 and downregulates membrane-bound KCC2 in phrenic motor neurons with chronic cervical SCI. However, 5 weeks post-C2SC, membrane-bound and cytosolic NKCC1 expression were not significantly affected by injury when analyzed separately, although the membrane/cytosolic ratio increased, consistent with net chloride influx. Membrane-bound and cytosolic KCC2 expression both increased when analyzed separately, although the membrane/cytosolic ratio decreased, consistent with net chloride efflux. Based on previous reports and our observations, cervical SCI may transiently disrupt cation-chloride cotransporter balance in phrenic motor neurons, but if that is the case, compensatory mechanisms must restore a normal NKCC1/KCC2 balance by 5 weeks post-injury (Cramer et al., 2008; Modol et al., 2014).

2. Materials and methods

2.1. Animals

All experimental procedures were approved by the Animal Care and Use Committee in the School of Veterinary Medicine at the University of Wisconsin. A total of 24 adult male Lewis rats were studied (11–12 weeks of age, Harlan, Indianapolis IN, Colony 202C). Rats were double-housed and maintained on a 12-hour light/dark cycle with access to food and water ad libitum.

2.2. Intrapleural injections

Anesthesia was induced with 2.5% isoflurane in 100% O_2, and then maintained via nose cone (2% isoflurane, 100% O_2). All rats were injected with Cholera toxin B fragment 7 days prior to spinal cord injury surgeries (0.2% w/v CtB; dissolved in sterile H_2O; Calbiochem, Billerica, MA). 12.5 μL of CtB was loaded into a 25 μL Hamilton syringe attached to a 9.52 mm sterile needle for bilateral injections (2 × 12.5 μL = 25 μL total per animal) at the 5th intercostal space at a depth of ~6 mm. This method was used to retrogradely label phrenic motor neurons (Mantilla et al., 2009). Following injections, isoflurane was discontinued, and rats were monitored for signs of respiratory compromise or distress (none observed).

2.3. Experimental groups

To investigate the effects of unilateral cervical spinal cord contusion (C2SC) on membrane-bound and cytosolic NKCC1 and KCC2 expression in phrenic motor neurons, rats were randomly assigned to the following groups: 1) sham (laminectomy; n = 12); and 2) C2SC (n = 12). Ipsilateral and contralateral changes in membrane-bound and cytosolic NKCC1 and KCC2 were analyzed in cervical segment 4 (C4) tissue sections from all animals in both groups.

2.4. Surgical preparation

Anesthesia and surgical preparation have been previously described (Navarrete-Opazo et al., 2017, 2015). Briefly, all rats were induced with isoflurane (5% isoflurane in 100% O_2), intubated using a flexible cannula inserted into the trachea, and mechanically ventilated (tidal volume 2.0–2.5 mL). Surgical plane of anesthesia was maintained with isoflurane at 2–2.5% in O_2 for the duration of the surgery and monitored by absence of toe pinch and palpebral responses. Oxygen saturation was monitored via pulse oximetry and body temperature was maintained at 36.5–37.5 °C using a rectal probe and external heating pad. All rats were injected subcutaneously 10–15 minutes before surgery with buprenorphine (0.05 mg/kg), carprofen (5 mg/kg), enrofloxacin (Baytril; 4 mg/kg) and sterile lactated Ringer's solution (10 mL; 5 mL per side) for pain management and anticipated fluid loss due to surgery.

2.5. Unilateral C2 spinal contusion

Following anesthetic induction and pre-operative surgical preparation, a dorsal cervical incision was made from the base of the skull to the C3 segment. The spinal cord was exposed at C2 via dorsal laminectomy. Unilateral contusions using the Infinite Horizons Impactor have been previously described (Alvarez-Argote et al., 2016; Rana et al., 2017). Briefly, the vertebral column was stabilized via 2 forceps connected to a base plate. Unilateral contusions were performed on the left side at the caudal end of the C2 spinal cord using a 1.3 mm diameter tip with the Infinite Horizons Impactor (135 kdyn, 0 s dwell time; Precision Systems and Instrumentation, LLC, Lexington, KY). After each contusion, probe force and displacement over time were displayed by the impactor. From the force and displacement over time output files, average maximum force, displacement, and impulse to the tissue per animal was determined. Following C2SC, overlying muscles were sutured, and the skin closed with stainless steel wound clips. All sham rats received a laminectomy but not a unilateral C2 contusion. The dura mater was left intact for all animals.

Post-operative care was provided at 6 h post-surgery, and twice per day (approximately every 12 h) after the first day post-surgery. Rats were housed in a heated incubator for 1-night post-surgery to ensure temperature regulation. Pain was managed by administering buprenorphine (0.05 mg/kg; 2×/day) subcutaneously for 3 days post-surgery, and carprofen one-day post-surgery (5 mg/kg; 1×/day). Enrofloxacin was also administered subcutaneously one-day post-surgery (Baytril; 4 mg/kg; 1×/day) to avoid possible gram-negative bacteria infection. Rats received subcutaneous injections of sterile lactated Ringer's solution (1–5 mL/day) and were manually fed a nutritional supplement (Diet Gel Boost; Clear H_2O; Westbrook, ME) until adequate volitional drinking and eating resumed. Nutritional supplement, chow, and long sipper water bottles were also provided near the bottom of home cages to ensure food and water was easily accessible to injured rats.

2.6. Tissue preparation

Five weeks post-injury, each animal was anesthetized and perfused intracardially with 0.1 M phosphate buffered saline (PBS), followed by paraformaldehyde (4% w/v in 0.1 M PBS, pH 7.4). The spinal cord was then removed from the vertebral column and post-fixed in paraformaldehyde overnight (4% w/v in 0.1 M PBS, pH 7.4). Spinal cord tissues were cryoprotected in 20% sucrose solution in 0.1 M PBS for 3 days, followed by 30% sucrose solution in 0.1 M PBS for 3 days. C3–5 spinal segments were then sliced transversely with individual tissues placed in sequentially numbered cell culture wells (tissue thickness: 40 μm) using a freezing microtome (Leica SM2000R, Buffalo Grove, IL)

and stored in antifreeze solution (30% glycerol, 30% ethylene glycol, 40% 0.1 M PBS, pH 7.4) at −20 °C until processed.

2.7. Immunolabeling

The T4 monoclonal NKCC antibody recognizes 310 residues of the C-terminus (760–1212) of both NKCC1 and NKCC2 isoforms (Lytle et al., 1995). The hybridoma culture supernatant containing the monoclonal antibody T4 (NKCC) was obtained from Developmental Studies Hybridoma Bank maintained by the University of Iowa (Department of Biological Sciences, Iowa City, IA). NKCC2 is not present in the spinal cord, so NKCC1 likely accounts for all spinal cord labeling (Gamba et al., 1994; Lytle et al., 1995). The T4 NKCC antibody was validated after its initial development (Lytle et al., 1995). The absence of staining has been shown in brain and brainstem tissue of NKCC1 -/- mice (Chen et al., 2005). The KCC2 (07-432) antibody has been validated and binds to residues 932-104 with no labeling in KCC2 knockdown mice (Blaesse et al., 2006; Williams et al., 1999). This antibody is also listed in the Journal of Comparative Neurology Antibody Registry. This KCC2 antibody has also been used in several CNS disease/trauma models and protein regulation studies (Horn et al., 2010; Lee et al., 2007). The antibody used against the Cholera toxin B subunit (227040, Calbiochem, Billerica, MA) recognizes the B subunit of Cholera toxin (CtB). Anti-CtB antibodies do not bind to any protein if CtB has not been introduced to the animal (Seven et al., 2018).

Immunofluorescence was used to examine the membrane and cytosolic expression of NKCC1 and KCC2, with CtB used as a marker for phrenic motor neurons. Tissue sections from C4 were used for immunolabeling because phrenic motor neurons are densely distributed in this region (Alvarez-Argote et al., 2016; Goshgarian and Rafols, 1981; Mantilla et al., 2009). As previously published, transverse tissue sections were numbered sequentially and every 8th section of cervical spinal cord segment 4 (C4; 40 µm) was used from each animal to evenly represent the entire C4 segment (Satriotomo et al., 2012). Thus, ~7 tissue sections were chosen from all animals in sham and C2SC groups and stained concurrently in a single batch to eliminate potential batch effects (sham n = 12 and C2SC n = 12). Triple labeling was used to visualize membrane and cytosolic expression of NKCC1 and KCC2 in CtB-positive phrenic motor neurons. After tissue sections were washed with 0.1 M TBS-Tween (0.2%), and incubated in blocking agent (normal donkey serum, Equitech-Bio SD32-0500), tissues were incubated in primary antibody raised against NKCC (mouse host, 1:1000, T4, AB_528406 Developmental Studies Hybridoma Bank, University of Iowa), KCC2 (rabbit host, 1:2000, Millipore 07-432), and CtB (goat host, 1:2500, Calbiochem 227-040) overnight at 4 °C. Tissues with primary antibody absent were also incubated overnight as controls. After washing with 0.1 M TBS-Tween (0.1%) tissues were incubated for 2 h at room temperature with secondary antibodies to label NKCC1, KCC2, and CtB (Alexa Fluor® 555 (A-31572), 488 (A-21206), 647 (A-21447), Invitrogen, Carlsbad, CA). Tissues with secondary antibody absent were also incubated as controls. Sections were mounted on charged slides using VectaShield Hardset mounting medium (Vector Laboratories, UK). A subset of tissue was stained with cresyl violet to visualize unilateral C2SC as previously published (Dougherty et al., 2016; Gonzalez-Rothi et al., 2015).

2.8. Image acquisition and analysis

All immunofluorescent tissues were imaged in z-series (2 µm step increments) using an Olympus spinning disk confocal microscope (Olympus IX81-DSU, Olympus Corp., Tokyo, Japan) with 20× magnification. For NKCC1, fluorescein isothiocyanate was used (FITC, 3 s, 35 gain). For KCC2, tetramethylrhodamine was used (TRITC, 5 s, 85 gain). For CtB, cyanine 5 was used (Cy5, 10 s, 255 gain). Neutral density was set to 1, and no binning was performed. Regions of interest for imaging were determined by CtB-positive cell labeling within the ventral horn of C4, signifying the phrenic motor nucleus. Two z-series images per tissue section were taken. One z-series image was taken on the left side (ipsilateral) and one on the right side (contralateral). The sides of the spinal cord were marked prior to tissue sectioning to ensure accurate side determination during imaging and analyses. ~14 images were analyzed per animal as ~7 tissue sections were stained. All images were collected with the same exposure and gain software settings.

Quantification of confocal immunofluorescent images was performed by analyzing CtB-labeled phrenic motor neurons within the ventral horn. Thresholds were determined using a custom adaptive thresholding algorithm in MATLAB (MathWorks, Natick, MA, USA). The adaptive threshold was calculated by first, constructing a pixel intensity histogram from the image. The pixel intensity corresponding to the 95th percentile was selected as the adaptive threshold to account for changes in CtB fluorescence intensities across animals and images. Using a fixed percentile threshold value would yield a higher threshold in an image with brighter signal and background fluorescence intensities, or a lower threshold in an image with dimmer signal and background fluorescence intensities. The pixels above the adaptive threshold (95th percentile across all pixel intensities) were considered CtB-positive. The coordinates of CtB-positive pixels/areas were used to measure fluorescence intensities of cytosolic NKCC1 and KCC2. KCC2 is robustly expressed on the cell membrane in adult neurons (Chamma et al., 2013; Li et al., 2007). Membrane-bound KCC2 expression was measured by first, determining the pixel-width of KCC2 membrane immunolabeling (~5 pixels) around CtB-labelled phrenic motor neurons. Then, we manually selected KCC2-positive membrane areas using high magnification images to measure pixel intensity. We used the same pixels/area to measure the pixel intensity corresponding to membrane-bound NKCC1. Background labeling was calculated by the median value of each channel and then subtracted from the respective measured cytosolic and membrane-bound protein intensities.

Two-way ANOVAs with the independent variables injury and side relative to injury were used to analyze all data sets (SAS JMP Inc, Cary, NC). Post-hoc analyses were performed with Tukey-Kramer honestly significant difference test. Differences were considered significant if $p < 0.05$. All data are displayed as mean ± sample standard deviation (SD).

3. Results

3.1. Characterization of contusion impact

Visualization of unilateral C2 contusions (C2SC) revealed similar injuries between injured animals (Fig. 1). The targeted C2SC force of 135 kdyn was delivered to the caudal end of C2. The average maximum force applied to the spinal cord was 139 ± 4 kdyn with an average displacement of 1020 ± 10 µm. The average impulse was 0.95 ± 0.03 kdyn sec and was calculated by integrating force data over

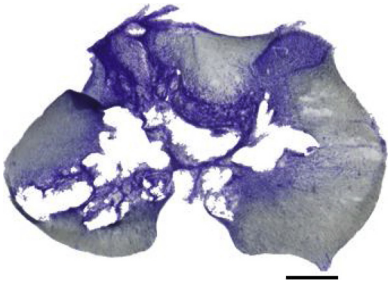

Fig. 1. Representative histology after unilateral cervical (C2) contusion (C2SC). Representative transverse C4 tissue segment (40 µm) labelled with cresyl violet after unilateral C2SC. White and grey matter pathology is evident on the ipsilateral (left) side, with some tissue damage spread to the contralateral side (right) despite unilateral impact. Scale bar: 500µm.

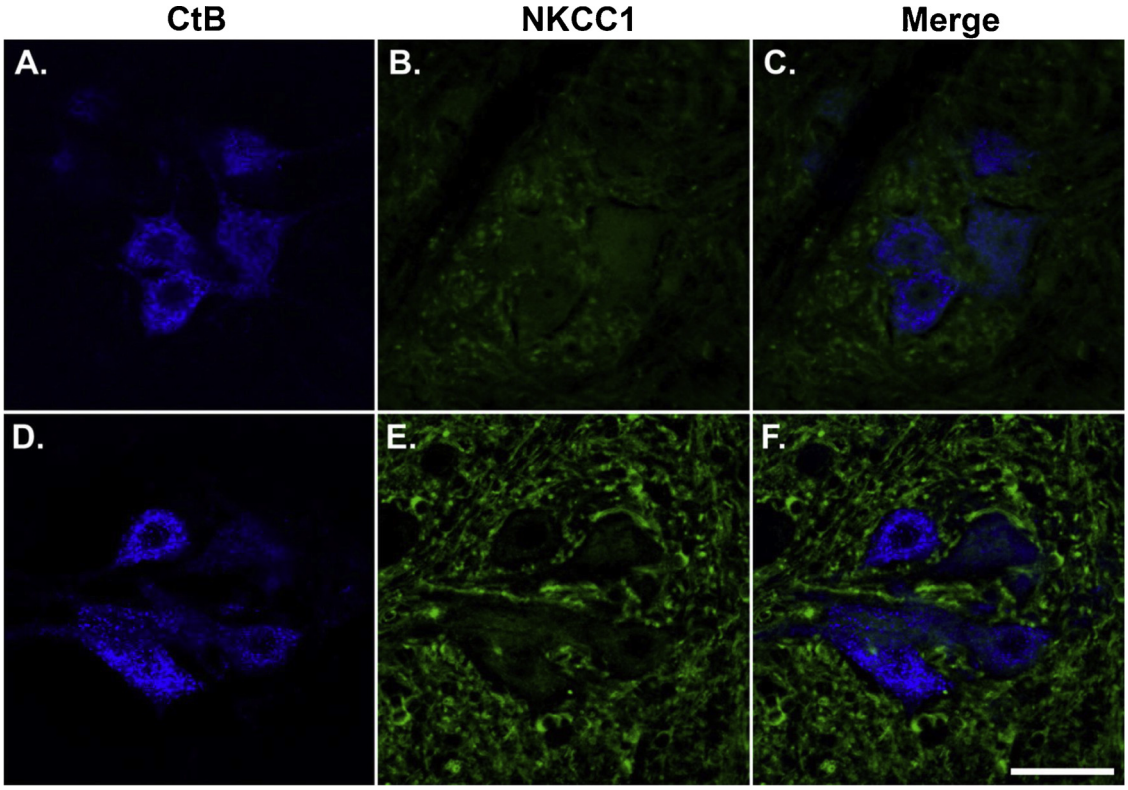

Fig. 2. NKCC1 membrane and cytosolic expression in phrenic motor neurons after unilateral cervical (C2) contusion (C2SC). A. Cholera toxin B fragment (CtB; blue) expression in retrogradely labelled phrenic motor neurons 5 weeks after sham (laminectomy) surgery. B. NKCC1 expression (green) in CtB-labeled phrenic motor neurons 5 weeks after sham surgery. C. Merged imaged of CtB and NKCC1 5 weeks after sham surgery. D. CtB (blue) expression in retrogradely labelled phrenic motor neurons 5 weeks after C2SC. E. NKCC1 expression (green) in CtB-labeled phrenic motor neurons 5 weeks after C2SC. F. Merged imaged of CtB and NKCC1 5 weeks after C2SC. Scale bar: 50 μm.

time using the output files from the Infinite Horizons Impactor. Deviation in maximum force values compared to desired force values are ˜5%. Minimal vertebral impact was evident in force-displacement traces.

3.2. Membrane-bound and cytosolic NKCC1 are not significantly affected by C2 contusion

Immunoreactivity revealed NKCC1 expression in CtB-labelled phrenic motor neurons in the ventral horn of cervical spinal segment 4 (C4) in both sham (laminectomy) and unilateral C2 contusion (C2SC) rats 5 weeks post-injury (Fig. 2). Membrane-bound NKCC1 expression was not significantly affected by C2SC at this time-point post-injury versus sham animals (mean ± SD in arbitrary units: sham ipsilateral = 282.10 ± 119.42; C2SC ipsilateral 329.80 ± 100.45; sham contralateral 279.53 ± 101.85; C2SC contralateral 331.35 ± 80.63; $p = 0.103$; Fig. 3). Cytosolic NKCC1 expression was not significantly affected by C2SC at this time-point post-injury versus sham animals (mean ± SD in arbitrary units: sham ipsilateral = 453.23 ± 269.77; C2SC ipsilateral = 351.52 ± 102.75; sham contralateral = 388.90 ± 225.06; C2SC contralateral = 361.43 ± 74.11; $p = 0.239$). We also analyzed the ratio of membrane-bound relative to cytosolic NKCC1 expression to normalize for rat to rat differences in staining intensity. Membrane-bound relative to cytosolic NKCC1 expression was increased after C2SC in phrenic motor neurons versus sham animals indicating a greater increase in membrane-bound NKCC1 compared to cytosolic expression, consistent with the trends observed when analyzing the compartments separately (mean ± SD in arbitrary units: sham ipsilateral = 0.69 ± 0.21; C2SC ipsilateral = 0.94 ± 0.14; sham contralateral = 0.76 ± 0.14; C2SC contralateral = 0.92 ± 0.10; $p < 0.001$; Figs. 2, 3). There was no difference in ipsilateral versus contralateral staining for membrane-bound, cytosolic, or membrane/cytosolic ratio, indicating that unilateral C2SC injuries affected both sides of the spinal cord equally (membrane-bound: $p = 0.987$; cytosol: $p = 0.618$; membrane-bound/cytosol ratio: $p = 0.614$; Fig. 3).

3.3. Membrane-bound and cytosolic KCC2 are increased after C2 contusion

Immunoreactivity revealed KCC2 expression in CtB-labelled phrenic motor neurons in the ventral horn of cervical spinal segment 4 (C4) in both sham (laminectomy) and unilateral C2SC rats 5 weeks post-injury (Fig. 4). Membrane-bound KCC2 expression increased in phrenic motor neurons after C2SC versus sham animals (mean ± SD in arbitrary units: sham ipsilateral = 316.01 ± 164.70; C2SC ipsilateral = 394.87 ± 72.12; sham contralateral = 323.27 ± 118.85; C2SC contralateral = 384.42 ± 86.10; $p = 0.045$; Fig. 5). Cytosolic KCC2 expression was also increased in phrenic motor neurons after C2SC versus sham animals (mean ± SD in arbitrary units: sham ipsilateral = 123.46 ± 55.84; C2SC ipsilateral = 216.00 ± 49.02; sham contralateral = 130.29 ± 71.79; C2SC contralateral = 228.38 ± 86.94; $p < 0.001$; Figs. 4, 5). We also analyzed the ratio of membrane-bound relative to cytosolic KCC2 expression to normalize for rat to rat differences in staining intensity. The ratio of membrane-bound to cytosolic KCC2 expression decreased in phrenic motor neurons after C2SC versus sham animals because of a greater increase in cytosolic expression relative to the smaller increase in membrane-bound expression (mean ± SD in arbitrary units: sham ipsilateral = 3.13 ± 2.51; C2SC ipsilateral = 1.88 ± 0.38; sham contralateral = 2.86 ± 1.27; C2SC contralateral = 1.87 ± 0.65; $p = 0.011$). There were no differences ipsilateral versus contralateral to injury when analyzing membrane-bound, cytosolic, or membrane/cytosolic ratio, indicating that C2SC affected both sides of the spinal cord equally (membrane-bound: $p = 0.963$;

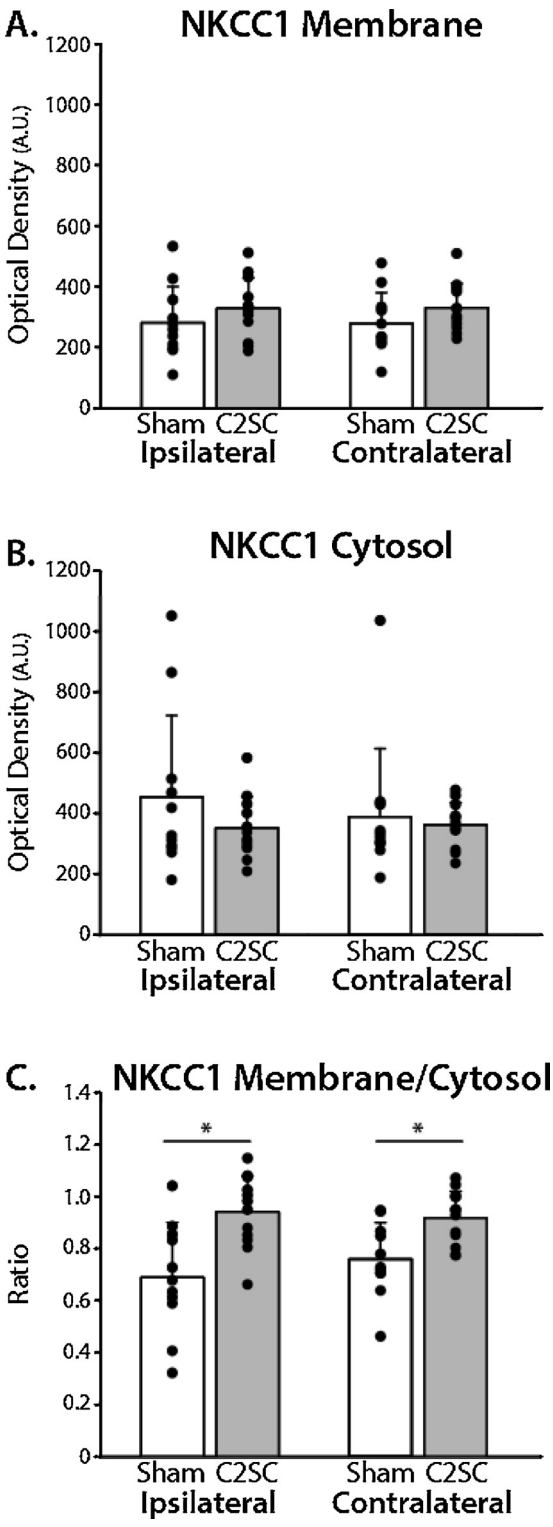

Fig. 3. Quantification of membrane-bound and cytosolic NKCC1 expression in phrenic motor neurons after unilateral cervical (C2) contusion. A. Membrane-bound NKCC1 in Cholera toxin B fragment (CtB) labeled phrenic motor neurons 5 weeks after sham (laminectomy, white bars) and unilateral cervical (C2) spinal contusion (C2SC, grey bars). Membrane-bound NKCC1 was not affected by C2SC on the ipsilateral or contralateral sides of the cervical spinal cord ($p = 0.103$ injury, $p = 0.987$ ipsi/contra effect) B. Cytosolic NKCC1 in CtB-labeled phrenic motor neurons 5 weeks after sham and C2SC. Cytosolic NKCC1 was not affected by C2SC on the ipsilateral or contralateral sides of the cervical spinal cord ($p = 0.239$ injury, $p = 0.618$ ipsi/contra effect). C. Ratio of membrane-bound and cytosolic NKCC1 in CtB-labeled phrenic motor neurons 5 weeks after sham and C2SC. Ratio of membrane-bound and cytosolic NKCC1 (membrane-bound/cytosolic NKCC1) was increased after C2SC compared to sham controls on the ipsilateral and contralateral sides of the cervical spinal cord ($p < 0.001$). There were no differences between ipsilateral and contralateral sides ($p = 0.614$ ipsi/contra). All data were analyzed using 2-way ANOVA with injury (sham vs. C2SC) and spinal cord side relative to injury (ipsilateral vs. contralateral) as variables. Tukey's HSD was used for post-hoc analysis when appropriate. All data are displayed as mean ± SD.

cytosol: $p = 0.633$; membrane-bound/cytosol ratio: $p = 0.735$, Fig. 5).

4. Discussion

Phrenic motor neurons receive excitatory and inhibitory synaptic input from medullary respiratory centers on a breath-by-breath basis. Whereas excitatory inputs drive breathing, inhibitory inputs sculpt (i.e. amplitude) and coordinate each breath (Zuperku and McCrimmon, 2002). In mature neurons, low $[Cl^-]_i$ and chloride-mediated hyperpolarization are maintained by the main chloride extruder, KCC2 (Ben-Ari et al., 1997; Payne et al., 2003; Rivera et al., 1999). Prior to the developmental switch, immature neurons contain high $[Cl^-]_i$ due to NKCC1-dependent chloride influx, resulting in chloride-mediated depolarization (Gao and Ziskind-Conhaim, 1995; Takahashi, 1984). Medullary respiratory nuclei undergo a developmental switch from chloride-mediated depolarization to hyperpolarization by embryonic day 19 (Ren and Greer, 2006). Thus, the functional balance of NKCC1 and KCC2 is necessary to regulate the strength and polarity of fast synaptic, chloride-dependent $GABA_A$- and glycinergic neurotransmission.

The balance of NKCC1 and KCC2 is plastic and can shift to favor high or low $[Cl^-]_i$ as observed during development or in disease such as spinal injury (Bos et al., 2013; Boulenguez et al., 2010; Kaila et al., 2014; Sanchez-Brualla et al., 2017). For example, ventral spinal KCC2 decreases in lumbar motor neurons after thoracic transection in adult and neonatal rats at acute time-points post-injury, contributing to SCI-induced spasticity (Bos et al., 2013; Boulenguez et al., 2010). After thoracic contusion, NKCC1 is upregulated and KCC2 downregulated in the lumbar spinal dorsal horn, contributing to neuropathic pain (Cramer et al., 2008). In these models, injury-induced NKCC1 and KCC2 dysregulation resemble expression patterns observed prior to the development switch (i.e. high NKCC1, low KCC2 (Ben-Ari et al., 1997; Rivera et al., 1999). In our model of incomplete cervical spinal contusion (C2SC), we do not see persistent downregulation of membrane-bound NKCC1 or KCC2 in phrenic motor neurons as reported at other time-points with different injury models (Bos et al., 2013; Boulenguez et al., 2010; Cramer et al., 2008).

Inhibitory synaptic transmission is necessary for appropriate inspiratory-expiratory phase transitions of the respiratory system (Tonkovic-Capin et al., 2003; Zuperku and McCrimmon, 2002). GABAergic mechanisms are critical for gain modulation of respiratory motor output, modifying breathing according to physiological demands. After injury, synaptic inputs in spared bulbospinal pathways to phrenic motor neurons may be amplified after loss of tonic GABA gain modulation, thereby minimizing impairment in tidal volume generation (Tonkovic-Capin et al., 2003; Zuperku and McCrimmon, 2002). A recent report suggests that NKCC1/KCC2 expression may shift to favor cell survival in conditions of injury or disease by reducing the energetic costs required to preserve low $[Cl^-]_i$ and maintain activity to promote recovery (Kaila et al., 2014). However, preserving excitability of respiratory motor neurons without regulation can lead to discoordinated breathing, muscle spasticity, and neuropathic pain via degraded chloride gradients (Bos et al., 2013; Boulenguez et al., 2010; Cramer et al., 2008). Here, we do not observe clear shifts in NKCC1/KCC2 balance in phrenic motor neurons 5 weeks post-C2SC. It is unclear if there was an imbalance acutely, as we measured NKCC1 and KCC2 at a

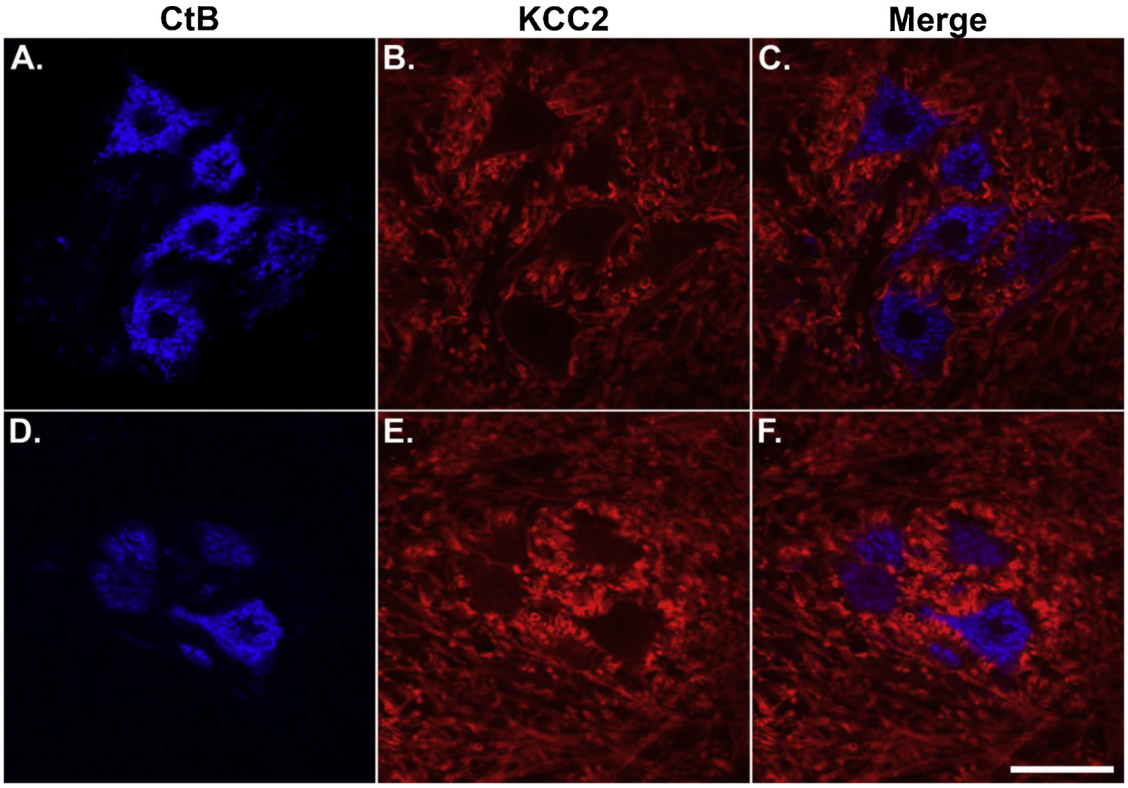

Fig. 4. KCC2 membrane and cytosolic expression in phrenic motor neurons after unilateral cervical (C2) contusion. A. Cholera toxin B fragment (CtB; blue) expression in retrogradely labelled phrenic motor neurons 5 weeks after sham (laminectomy) surgery. B. KCC2 expression (red) in CtB-labeled phrenic motor neurons 5 weeks after sham surgery. C. Merged imaged of CtB and KCC2 5 weeks after sham surgery. D. CtB (blue) expression in retrogradely labelled phrenic motor neurons 5 weeks after C2SC. E. KCC2 expression (red) in CtB-labeled phrenic motor neurons 5 weeks after C2SC. F. Merged imaged of CtB and KCC2 5 weeks after C2SC. Scale bar: 50 μm.

single time-point. However, we do observe an increase in cytosolic KCC2, which may suggest regulatory mechanisms are working to drive functional KCC2 to the membrane to compensate for transient disruption.

Our original hypothesis that NKCC1/KCC2 balance is dysregulated by incomplete cervical spinal injury in phrenic motor neurons 5 weeks post-injury was not supported by our observations. At 5 weeks post-injury, membrane-bound and cytosolic NKCC1 expression were not significantly different in phrenic motor neurons in C2SC versus sham rats when analyzed separately. However, when analyzing the membrane/cytosolic ratio, we observed a significant increase indicating that membrane-bound NKCC1 was relatively greater with respect to cytosolic expression. This expression profile would be consistent with a net increase in chloride influx. We observed increased membrane-bound and cytosolic KCC2 expression in phrenic motor neurons in C2SC versus sham rats when analyzed separately. However, when analyzing the membrane/cytosolic ratio, we observed a significant decrease due to a larger increase in cytosolic relative to the increase in membrane-bound expression. Thus, it appears that incomplete C2SC exerts complex effects on NKCC1/KCC2 balance in phrenic motor neurons. If there was dysregulation in NKCC1 or KCC2 expression in phrenic motor neurons, as has been shown in other motor pools, we do not observe that clear shift using this injury model. If NKCC1/KCC2 imbalance occurred acutely in phrenic motor neurons after C2SC, the functional (i.e. membrane-bound) balance of NKCC1/KCC2 was already restored, and actually exceeded sham levels, at 5 weeks post-injury.

During development, inhibitory synaptic transmission within the respiratory network matures earlier than many other motor systems because it must be functional at birth (Brockhaus and Ballanyi, 1998; Ren and Greer, 2006; Watanabe and Fukuda, 2015). If NKCC1 and KCC2 are dysregulated acutely post-injury, eventual restoration of membrane-bound NKCC1 and KCC2 balance may be needed to restore normal respiratory function. Equal impact of the ipsilateral and contralateral sides suggests that both sides of the spinal cord were affected equally, despite lateralized injuries. Further, regulatory mechanisms affecting the NKCC1/KCC2 balance post-injury are not directly impacted by the injury *per se*.

The increased ratio of membrane-bound to cytosolic NKCC1 after C2SC suggests that the impact of C2SC on NKCC1 is relatively small, or that powerful compensatory mechanisms had normalized, and even exceeded, cytosolic and membrane-bound NKCC1 expression and function by 5 weeks post-injury. Although both membrane-bound and cytosolic KCC2 increased post-C2SC, the membrane/cytosolic ratio actually decreased because the membrane-bound effects were smaller. We suggest that the increase in cytosolic KCC2 expression reflects compensatory gene expression, increasing KCC2 protein expression and providing the substrate for KCC2 translocation to the cell membrane. Such transient changes are reported in the spinal dorsal horn with a similar time-course post-injury (24). Collectively, these data support the idea that unilateral C2SC exerts complex effects on the NKCC1/KCC2 balance in phrenic motor neurons in adult rats.

4.1. NKCC1 and KCC2 expression in phrenic motor neurons

Five weeks post-injury we did not see clear membrane-bound KCC2 downregulation and NKCC1 upregulation as has been reported by others assessing other motor pools at acute time-points post-injury. For example, recent reports indicate that NKCC1 and KCC2 undergo transient, time-dependent dysregulation after spinal or peripheral nerve injuries. After thoracic contusions, NKCC1 is upregulated by 60% and KCC2 is downregulated by 40% within the injury epicenter 14 days post-injury, with no NKCC1 or KCC2 expression changes rostral to the

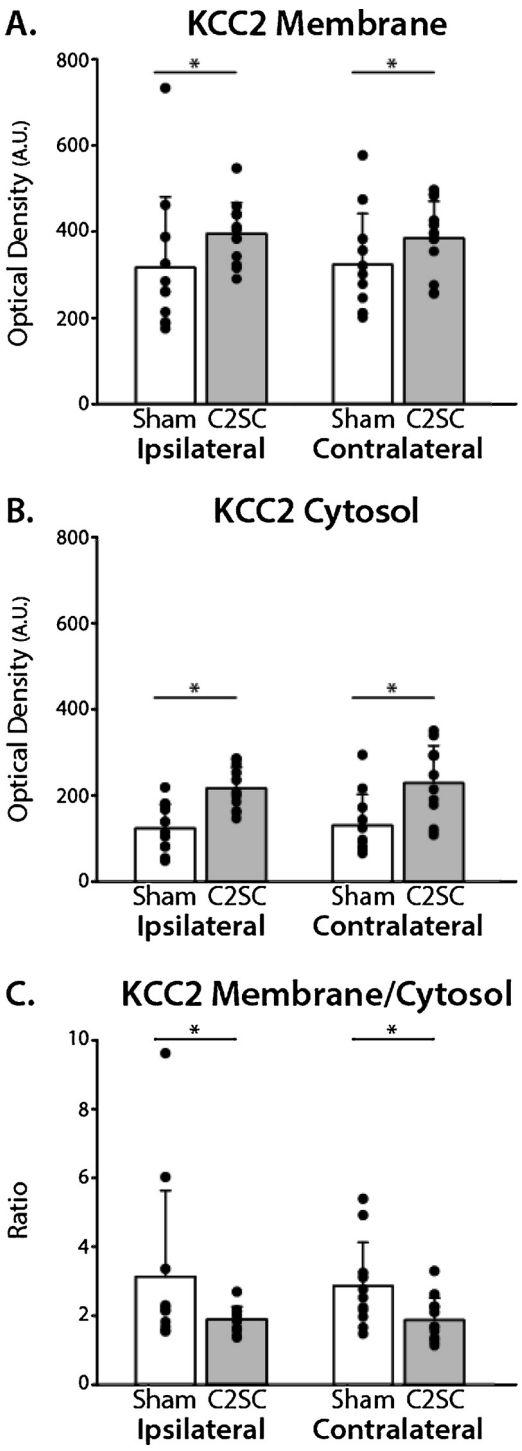

Fig. 5. Quantification of membrane-bound and cytosolic KCC2 expression in phrenic motor neurons after unilateral cervical (C2) contusion. A. Membrane-bound KCC2 in Cholera toxin B fragment (CtB) labeled phrenic motor neurons 5 weeks after sham (laminectomy, white bars) and cervical (C2) spinal contusion (C2SC, grey bars). Membrane-bound KCC2 was increased after C2SC on the ipsilateral and contralateral sides of the cervical spinal cord ($p = 0.045$ injury effect). There were no differences between ipsilateral and contralateral sides ($p = 0.963$ ipsi/contra effect). B. Cytosolic KCC2 in CtB-labeled phrenic motor neurons 5 weeks after sham and C2SC. Cytosolic KCC2 was increased after C2SC on the ipsilateral and contralateral sides of the cervical spinal cord ($p < 0.001$ injury effect). There were no differences between ipsilateral and contralateral sides ($p = 0.633$ ipsi/contra effect). C. Ratio of membrane-bound and cytosolic KCC2 (membrane-bound/cytosolic KCC2) in CtB-labeled phrenic motor neurons 5 weeks after sham and C2SC. Ratio of membrane-bound to cytosolic KCC2 was decreased after C2SC compared to sham controls on the ipsilateral and contralateral sides of the cervical spinal cord ($p = 0.011$ injury effect). There were no differences between ipsilateral and contralateral sides ($p = 0.735$ ipsi/contra effect). All data were analyzed using 2-way ANOVA with injury (sham vs. C2SC) and spinal cord side relative to injury (ipsilateral vs. contralateral). Tukey's HSD was used for post-hoc analysis when appropriate. All data are displayed as mean ± SD.

lesion (Cramer et al., 2008). Here, membrane-bound and cytosolic NKCC1 and KCC2 measurements were made at C4, caudal to unilateral C2 spinal contusion injuries to determine phrenic motor neuron expression. Thus, it is possible that NKCC1/KCC2 dysregulation is more apparent near the injury site. Another recent study also reported transient changes in NKCC1 and KCC2 expression following sciatic nerve injury. NKCC1 rapidly increased in dorsal root ganglia, while KCC2 decreased in the spinal dorsal horn; however, both returned to control levels by 28 days post-injury (Modol et al., 2014). These data are consistent with NKCC1/KCC2 regulation and normalization after only a few weeks post-injury as reported here.

Time-dependent NKCC1 and KCC2 regulation with spinal injury, chronic pain, or with epilepsy have generally been performed in short time frames (< 4 weeks; (Bos et al., 2013). After spinal injury, there is time-dependent dysfunction and compensation in the respiratory network. Analyzing protein expression acutely after spinal injury helps understand cellular mechanisms directly resulting from trauma. Studies with chronic injury are critical to understand compensation and plasticity beyond the acute phase. For example, cervical spinal hemisection disrupts medullary serotonergic innervation of the phrenic motor nucleus 2 weeks post-injury, and only partially recovers by 8 weeks post-injury (Golder and Mitchell, 2005). Spinal serotonin receptor activation and BDNF/TrkB signaling are critical for some potential mechanisms of compensatory respiratory plasticity following spinal cord injury (Golder and Mitchell, 2005; Lovett-Barr et al., 2012). Since serotonin 2 A and BDNF/TrkB signaling upregulate membrane-bound KCC2 in motor neurons following complete spinal transection (Bos et al., 2013; Sanchez-Brualla et al., 2017), we reasoned that serotonin/BDNF-dependent regulation of NKCC1 and KCC2 would be diminished with acute injury (< 2 weeks) due to axotomy of descending serotonergic neurons. We predicted that dysregulation of NKCC1 and KCC2 expression would be observed in phrenic motor neurons for at least up to 5 weeks post-injury because important signaling pathways that regulate the functional balance of NKCC1/KCC2 are not fully restored at 8 weeks post-injury (Golder and Mitchell, 2005). Since then, several reports indicate that their balance is disrupted with shorter times post-injury but is already restored by 5 weeks (Cramer et al., 2008; Modol et al., 2014). Because of our experimental design, we remain uncertain if NKCC1/KCC2 are dysregulated in phrenic motor neurons at earlier times post-injury, or if C2 contusion injuries are even sufficient to cause such an effect.

The reported recycling speed of membrane-bound NKCC1 and KCC2 is remarkably fast (˜10 min; (Kaila et al., 2014; Lee et al., 2007) and functional chloride-dependent synaptic inhibition is critical. Thus, it is possible that regulatory mechanisms work quickly to restore

membrane-bound NKCC1/KCC2 balance. This is particularly important in phrenic motor neurons since their activity is necessary for normal breathing. Interestingly, our data show that cytosolic KCC2 was upregulated 5 weeks post-injury, consistent with regulatory mechanisms working to achieve NKCC1/KCC2 balance in phrenic motor neurons, and may signify increased KCC2 membrane trafficking (Bos et al., 2013). Because we did not see dysregulation of NKCC1 and KCC2, membrane-bound expression of NKCC1 and KCC2 may be tightly regulated in respiratory motor neurons. In development, chloride-dependent hyperpolarization is established in medullary respiratory nuclei in advance of other CNS regions, suggesting that chloride-mediated conductance is tightly regulated in this neural network because adequate respiratory function is critical to survival (Brockhaus and Ballanyi, 1998; Ren and Greer, 2006).

Here, we assessed NKCC1 and KCC2 expression in phrenic motor neurons after unilateral C2SC. Although we observed ipsilateral forepaw clenching in C2SC animals, we did not test forelimb grip strength or exploratory function. This may have allowed for stratification by recovery rate of forepaw strength. After moderately severe contusion injuries, rats regain forelimb function and compensate rapidly (Anderson et al., 2009; Lane et al., 2012). Thus, it is possible that functional deficits observed from digit/wrist flexion would have allowed stratification with a mild contusion (135 kdyn) at this time post-injury, although we suspect this would be limited (Anderson et al., 2009). In other models of injury, muscle spasticity and neuropathic pain are linked to NKCC1 and KCC2 dysregulation (Boulenguez et al., 2010; Cramer et al., 2008). We did not assess neuropathic pain or diaphragm spasticity. Pairing physiological measurements with NKCC1 and KCC2 expression patterns would allow correlation of NKCC1 and KCC2 expression with important physiological outcomes; however, this was beyond the scope of this study.

Spinal disinhibition caused by spinal injury has been reported in motor behaviors, including respiration and locomotion in people and rodents with spinal cord injury (Bos et al., 2013; Boulenguez et al., 2010; Laffont et al., 2003; Silver and Lehr, 1981). In rodent injury models, KCC2 downregulation has a physiological cost, similar to NKCC1 upregulation with acute injury; maladaptive hyperexcitability including epilepsy and discoordinated movement like sporadic diaphragm activation during expiration (i.e. spasticity). This may be a regulatory response to partially compensate for loss of cell excitability, preserve activity and reduce energy expenditure needed to maintain a low $[Cl^-]_i$ (Kaila et al., 2014). However, compensation may come at the cost of muscle dyscoordination, such as sporadic diaphragm activation during expiration (Laffont et al., 2003; Silver and Lehr, 1981).

5. Conclusion

These data are consistent with transient, cation-chloride cotransporter dysregulation shown in other models of spinal and peripheral injury. These data show that NKCC1 and KCC2 are present on phrenic motor neurons and may respond with transient dysregulation after spinal injury. This is the first insight into the plastic potential of cation-chloride cotransporters in phrenic motor neurons after unilateral cervical spinal contusion injury and may serve as a launching point for other studies aiming to investigate the impact of chloride-dependent synaptic inhibition in the acute phase post-injury on breathing and breathing recovery after spinal cord injury.

Acknowledgements

This work was supported by the Department of Defense (CDMRP SC120226), and the National Institutes of Health (HL69064, OT2OD023854, and HL105511). L. Allen was supported by a Science and Medicine Graduate Research Fellowship and NICHD (T32-HD043730). The authors thank Kendra Braegelmann and Joel Weltman for their assistance with animal maintenance, and Raphael Perim for his assistance with figures. The authors declare no competing financial interests.

References

Alvarez-Argote, S., Gransee, H.M., Mora, J.C., Stowe, J.M., Jorgenson, A.J., Sieck, G.C., Mantilla, C.B., 2016. The Impact of Midcervical Contusion Injury on Diaphragm Muscle Function. J. Neurotrauma 33, 500–509.

Anderson, K.D., Sharp, K.G., Hofstadter, M., Irvine, K.A., Murray, M., Steward, O., 2009. Forelimb locomotor assessment scale (FLAS): novel assessment of forelimb dysfunction after cervical spinal cord injury. Exp. Neurol. 220, 23–33.

Ben-Ari, Y., Khazipov, R., Leinekugel, X., Caillard, O., Gaiarsa, J.L., 1997. GABAA, NMDA and AMPA receptors: a developmentally regulated' menage a trois'. Trends Neurosci. 20, 523–529.

Blaesse, P., Guillemin, I., Schindler, J., Schweizer, M., Delpire, E., Khiroug, L., Friauf, E., Nothwang, H.G., 2006. Oligomerization of KCC2 correlates with development of inhibitory neurotransmission. J. Neurosci. 26, 10407–10419.

Bos, R., Sadlaoud, K., Boulenguez, P., Buttigieg, D., Liabeuf, S., Brocard, C., Haase, G., Bras, H., Vinay, L., 2013. Activation of 5-HT2A receptors upregulates the function of the neuronal K-Cl cotransporter KCC2. Proc. Natl. Acad. Sci. U. S. A. 110, 348–353.

Boulenguez, P., Liabeuf, S., Bos, R., Bras, H., Jean-Xavier, C., Brocard, C., Stil, A., Darbon, P., Cattaert, D., Delpire, E., Marsala, M., Vinay, L., 2010. Down-regulation of the potassium-chloride cotransporter KCC2 contributes to spasticity after spinal cord injury. Nat. Med. 16, 302–307.

Britton, D., Goldstein, B., Jones-Redmond, J., Esselman, P., 2005. Baclofen pump intervention for spasticity affecting pulmonary function. J. Spinal Cord Med. 28, 343–347.

Brockhaus, J., Ballanyi, K., 1998. Synaptic inhibition in the isolated respiratory network of neonatal rats. Eur. J. Neurosci. 10, 3823–3839.

Chamma, I., Heubl, M., Chevy, Q., Renner, M., Moutkine, I., Eugene, E., Poncer, J.C., Levi, S., 2013. Activity-dependent regulation of the K/Cl transporter KCC2 membrane diffusion, clustering, and function in hippocampal neurons. J. Neurosci. 33, 15488–15503.

Chen, H., Luo, J., Kintner, D.B., Shull, G.E., Sun, D., 2005. Na(+)-dependent chloride transporter (NKCC1)-null mice exhibit less gray and white matter damage after focal cerebral ischemia. J. Cereb. Blood Flow Metab. 25, 54–66.

Cohen, I., Navarro, V., Clemenceau, S., Baulac, M., Miles, R., 2002. On the origin of interictal activity in human temporal lobe epilepsy in vitro. Science 298, 1418–1421.

Coull, J.A., Boudreau, D., Bachand, K., Prescott, S.A., Nault, F., Sik, A., De Koninck, P., De Koninck, Y., 2003. Trans-synaptic shift in anion gradient in spinal lamina I neurons as a mechanism of neuropathic pain. Nature 424, 938–942.

Cramer, S.W., Baggott, C., Cain, J., Tilghman, J., Allcock, B., Miranpuri, G., Rajpal, S., Sun, D., Resnick, D., 2008. The role of cation-dependent chloride transporters in neuropathic pain following spinal cord injury. Mol. Pain 4, 36.

Delpire, E., Mount, D.B., 2002. Human and murine phenotypes associated with defects in cation-chloride cotransport. Annu. Rev. Physiol. 64, 803–843.

Dougherty, B.J., Gonzalez-Rothi, E.J., Lee, K.Z., Ross, H.H., Reier, P.J., Fuller, D.D., 2016. Respiratory outcomes after mid-cervical transplantation of embryonic medullary cells in rats with cervical spinal cord injury. Exp. Neurol. 278, 22–26.

Frankel, H.L., Coll, J.R., Charlifue, S.W., Whiteneck, G.G., Gardner, B.P., Jamous, M.A., Krishnan, K.R., Nuseibeh, I., Savic, G., Sett, P., 1998. Long-term survival in spinal cord injury: a fifty year investigation. Spinal Cord 36, 266–274.

Gamba, G., Miyanoshita, A., Lombardi, M., Lytton, J., Lee, W.S., Hediger, M.A., Hebert, S.C., 1994. Molecular cloning, primary structure, and characterization of two members of the mammalian electroneutral sodium-(potassium)-chloride cotransporter family expressed in kidney. J. Biol. Chem. 269, 17713–17722.

Gao, B.X., Ziskind-Conhaim, L., 1995. Development of glycine- and GABA-gated currents in rat spinal motoneurons. J. Neurophysiol. 74, 113–121.

Golder, F.J., Mitchell, G.S., 2005. Spinal synaptic enhancement with acute intermittent hypoxia improves respiratory function after chronic cervical spinal cord injury. J. Neurosci. 25, 2925–2932.

Gonzalez-Rothi, E.J., Rombola, A.M., Rousseau, C.A., Mercier, L.M., Fitzpatrick, G.M., Reier, P.J., Fuller, D.D., Lane, M.A., 2015. Spinal interneurons and forelimb plasticity after incomplete cervical spinal cord injury in adult rats. J. Neurotrauma 32, 893–907.

Goshgarian, H.G., Rafols, J.A., 1981. The phrenic nucleus of th albino rat: a correlative HRP and Golgi study. J. Comp. Neurol. 201, 441–456.

Hasbargen, T., Ahmed, M.M., Miranpuri, G., Li, L., Kahle, K.T., Resnick, D., Sun, D., 2010. Role of NKCC1 and KCC2 in the development of chronic neuropathic pain following spinal cord injury. Ann. N. Y. Acad. Sci. 1198, 168–172.

Hebert, S.C., Mount, D.B., Gamba, G., 2004. Molecular physiology of cation-coupled Cl-cotransport: the SLC12 family. Pflugers Arch. 447, 580–593.

Horn, Z., Ringstedt, T., Blaesse, P., Kaila, K., Herlenius, E., 2010. Premature expression of KCC2 in embryonic mice perturbs neural development by an ion transport-independent mechanism. Eur. J. Neurosci. 31, 2142–2155.

Kaila, K., Price, T.J., Payne, J.A., Puskarjov, M., Voipio, J., 2014. Cation-chloride cotransporters in neuronal development, plasticity and disease. Nat. Rev. Neurosci. 15, 637–654.

Laffont, I., Durand, M.C., Rech, C., De, La, Sotta, A.P., Hart, N., Dizien, O., Lofaso, F., 2003. Breathlessness associated with abdominal spastic contraction in a patient with C4 tetraplegia: a case report. Arch. Phys. Med. Rehabil. 84, 906–908.

Lane, M.A., Lee, K.Z., Salazar, K., O'Steen, B.E., Bloom, D.C., Fuller, D.D., Reier, P.J., 2012. Respiratory function following bilateral mid-cervical contusion injury in the adult rat. Exp. Neurol. 235, 197–210.

Lee, H.H., Walker, J.A., Williams, J.R., Goodier, R.J., Payne, J.A., Moss, S.J., 2007. Direct

protein kinase C-dependent phosphorylation regulates the cell surface stability and activity of the potassium chloride cotransporter KCC2. J. Biol. Chem. 282, 29777–29784.
Li, H., Khirug, S., Cai, C., Ludwig, A., Blaesse, P., Kolikova, J., Afzalov, R., Coleman, S.K., Lauri, S., Airaksinen, M.S., Keinanen, K., Khiroug, L., Saarma, M., Kaila, K., Rivera, C., 2007. KCC2 interacts with the dendritic cytoskeleton to promote spine development. Neuron 56, 1019–1033.
Lovett-Barr, M.R., Satriotomo, I., Muir, G.D., Wilkerson, J.E., Hoffman, M.S., Vinit, S., Mitchell, G.S., 2012. Repetitive intermittent hypoxia induces respiratory and somatic motor recovery after chronic cervical spinal injury. J. Neurosci. 32, 3591–3600.
Lytle, C., Xu, J.C., Biemesderfer, D., Forbush 3rd, B., 1995. Distribution and diversity of Na-K-Cl cotransport proteins: a study with monoclonal antibodies. Am. J. Physiol. 269, C1496–1505.
Mantilla, C.B., Zhan, W.Z., Sieck, G.C., 2009. Retrograde labeling of phrenic motoneurons by intrapleural injection. J. Neurosci. Methods 182, 244–249.
Modol, L., Cobianchi, S., Navarro, X., 2014. Prevention of NKCC1 phosphorylation avoids downregulation of KCC2 in central sensory pathways and reduces neuropathic pain after peripheral nerve injury. Pain 155, 1577–1590.
Nabekura, J., Ueno, T., Okabe, A., Furuta, A., Iwaki, T., Shimizu-Okabe, C., Fukuda, A., Akaike, N., 2002. Reduction of KCC2 expression and GABAA receptor-mediated excitation after in vivo axonal injury. J. Neurosci. 22, 4412–4417.
Navarrete-Opazo, A., Vinit, S., Dougherty, B.J., Mitchell, G.S., 2015. Daily acute intermittent hypoxia elicits functional recovery of diaphragm and inspiratory intercostal muscle activity after acute cervical spinal injury. Exp. Neurol. 266, 1–10.
Navarrete-Opazo, A., Dougherty, B.J., Mitchell, G.S., 2017. Enhanced recovery of breathing capacity from combined adenosine 2A receptor inhibition and daily acute intermittent hypoxia after chronic cervical spinal injury. Exp. Neurol. 287, 93–101.
NSCISC, 2018. The University of Alabama at Birmingham: National Spinal Cord Injury Statistical Center.
Payne, J.A., 1997. Functional characterization of the neuronal-specific K-Cl cotransporter: implications for [K+]o regulation. Am. J. Physiol. 273, C1516–1525.
Payne, J.A., Rivera, C., Voipio, J., Kaila, K., 2003. Cation–chloride co-transporters in neuronal communication, development and trauma. Trends Neurosci. 26, 199–206.
Price, T.J., Cervero, F., Gold, M.S., Hammond, D.L., Prescott, S.A., 2009. Chloride regulation in the pain pathway. Brain Res. Rev. 60, 149–170.
Rana, S., Sieck, G.C., Mantilla, C.B., 2017. Diaphragm electromyographic activity following unilateral midcervical contusion injury in rats. J. Neurophysiol. 117, 545–555.
Ren, J., Greer, J.J., 2006. Modulation of respiratory rhythmogenesis by chloride-mediated conductances during the perinatal period. J. Neurosci. 26, 3721–3730.
Rivera, C., Voipio, J., Payne, J.A., Ruusuvuori, E., Lahtinen, H., Lamsa, K., Pirvola, U., Saarma, M., Kaila, K., 1999. The K+/Cl- co-transporter KCC2 renders GABA hyperpolarizing during neuronal maturation. Nature 397, 251–255.
Sanchez-Brualla, I., Boulenguez, P., Brocard, C., Liabeuf, S., Viallat-Lieutaud, A., Navarro, X., Udina, E., Brocard, F., 2017. Activation of 5-HT2A receptors restores KCC2 function and reduces neuropathic pain after spinal cord injury. Neuroscience 387, 48–57.
Satriotomo, I., Dale, E.A., Dahlberg, J.M., Mitchell, G.S., 2012. Repetitive acute intermittent hypoxia increases expression of proteins associated with plasticity in the phrenic motor nucleus. Exp. Neurol. 237, 103–115.
Seven, Y.B., Perim, R.R., Hobson, O.R., Simon, A.K., Tadjalli, A., Mitchell, G.S., 2018. Phrenic motor neuron adenosine 2A receptors elicit phrenic motor facilitation. J. Physiol. 596, 1501–1512.
Silver, J.R., Lehr, R.P., 1981. Dyspnoea during generalised spasms in tetraplegic patients. J. Neurol. Neurosurg. Psychiatry 44, 842–845.
Takahashi, T., 1984. Inhibitory miniature synaptic potentials in rat motoneurons. Proc. R. Soc. Lond. B Biol. Sci. 221, 103–109.
Tonkovic-Capin, V., Stucke, A.G., Stuth, E.A., Tonkovic-Capin, M., Hopp, F.A., McCrimmon, D.R., Zuperku, E.J., 2003. Differential processing of excitation by GABAergic gain modulation in canine caudal ventral respiratory group neurons. J. Neurophysiol. 89, 862–870.
Viemari, J.C., Bos, R., Boulenguez, P., Brocard, C., Brocard, F., Bras, H., Coulon, P., Liabeuf, S., Pearlstein, E., Sadlaoud, K., Stil, A., Tazerart, S., Vinay, L., 2011. Chapter 1–importance of chloride homeostasis in the operation of rhythmic motor networks. Prog. Brain Res. 188, 3–14.
Watanabe, M., Fukuda, A., 2015. Development and regulation of chloride homeostasis in the central nervous system. Front. Cell. Neurosci. 9, 371.
Williams, J.R., Sharp, J.W., Kumari, V.G., Wilson, M., Payne, J.A., 1999. The neuron-specific K-Cl cotransporter, KCC2. Antibody development and initial characterization of the protein. J. Biol. Chem. 274, 12656–12664.
Winslow, C., Rozovsky, J., 2003. Effect of spinal cord injury on the respiratory system. Am. J. Phys. Med. Rehabil. 82, 803–814.
Zuperku, E.J., McCrimmon, D.R., 2002. Gain modulation of respiratory neurons. Respir. Physiol. Neurobiol. 131, 121–133.